Phyton-
International Journal of
Experimental Botany

Tech Science Press

DOI: 10.32604/phyton.2024.057518

ARTICLE

Encapsulation of Clove Oil Nanoemlusion in Chitosan-Based Nano-Composite: *In Vitro* and *in Vivo* Antifungal Activity against *Rhizoctonia solani* and *Sclerotium rolfsii*

Ahmed Mahmoud Ismail[1,2,3,*], Eman Said Elshewy[3], Isra H. Ali[4,5], Naglaa Abd Elbaki Sallam Muhanna[3] and Eman Yehia Khafagi[3]

[1]Department of Arid Land Agriculture, College of Agricultural and Food Sciences, King Faisal University, Al-Ahsa, 31982, Saudi Arabia

[2]Pests and Plant Diseases Unit, College of Agricultural and Food Sciences, King Faisal University, Al-Ahsa, 31982, Saudi Arabia

[3]Vegetable Diseases Research Department, Plant Pathology Research Institute, Agricultural Research Center (ARC), Giza, 12619, Egypt

[4]Department of Pharmaceutics, Faculty of Pharmacy, University of Sadat City, Sadat City, 32958, Egypt

[5]Nanomedicine Laboratory, Faculty of Pharmacy, University of Sadat City, Sadat City, 32958, Egypt

Corresponding Author: Ahmed Mahmoud Ismail. Email: amismail@kfu.edu.sa

Received: 20 August 2024 Accepted: 10 October 2024 Published: 30 November 2024

ABSTRACT

Rhizoctonia solani Kühn and *Sclerotium rolfsii* Sacc. are the primary soil-borne plant diseases responsible for significant reductions in global crop yields. The primary goal of this study was to investigate the antifungal potentials of clove essential oil (CEO), nanoemulsion form (CEONE) and chitosan/nanoemulsion nanocomposite (CS/CEONE) against *R. solani* and *S. rolfsii* through *in vitro* and *in vivo* trials. Both CEONE and CS/CEONE were prepared and investigated for their physical chemical and morphological characterization. The poisoned medium method was utilized to evaluate the inhibitory effects of CEO, CEONE and CS/CEONE on the mycelial growth and enzymatic activity of *R. solani* and *S. rolfsii*. The changes of hyphae of *R. solani* and *S. rolfsii* in response to treating with CEONE and CS/CEONE were observed with scanning electron microscope (SEM). The results revealed that CEONE have larger size 86 ± 3 nm and a broader range of PDI 0.121 ± 0.011 on the average. While, CS/CEONE has smaller size of 49 ± 4 nm and narrower PDI of 0.099 ± 0.009. Both nanoemulsions had uniform spherical nanodroplets form and exhibited acidic nature. Fourier Transform Infrared Spectroscopy (FTIR) and UV-Visible Spectroscopy (UV-Vis) verified the successful incorporation of both CS and CEO within the nanoemulsion system. The results demonstrated a sustained and prolonged release profile from CS/CEONE for up to 4 days. The inhibitory effect of CEONE and CS/CEONE showed dose-dependent activity against mycelial growth of both fungi. CEONE and CS/CEONE at concentration 500 µL/L exhibited the strongest inhibition with a significant ($p < 0.05$) variation among them with value ranging from 56.11% to 71.94% and 52.2% to 79.2%, respectively. Comparing to control, CS/CEONE revealed the highest inhibitory effect against *S. rolfsii* after 96 h followed by CEONE with value reached 50.6% and 44.1%, respectively. The antifungal activity of the nanoemulsion showed strain–dependent behavior, where *S. rolfsii* was the most affected. SEM images showed changes in the hyphal structure of *S. rolfsii* and *R. solani* resulting from the impact of CEONE and CS/CEONE. Activity of pectinase and cellulase secreted by both fungi was also negatively affected by CEO, CEONE and CS/CEONE at all tested concentrations. Greenhouse trials revealed that increasing the concentrations of CEO, CEONE, and CS/CEONE from 50 to 500 µL/L gradually increased their effectiveness in reducing the DI% and DS% of black scurf, stem

canker, pre-damping off, and post-damping off diseases on potato. The results suggest that incorporation of CS to CEONE enhanced its activity and can be utilized as a secure and non-toxic nanocomposite.

KEYWORDS

Black scurf; chitosan; clove oil; damping-off; inhibitory; nanocomposite; nanoemulsion; stem canker

1 Introduction

Under both open field and greenhouse conditions, *Sclerotium rolfsii* Sacc. and *Rhizoctonia solani* Kühn are the main soil-borne plant pathogens responsible for causing economically substantial plant diseases, like brown blotches, black scurf, seedling wilting, and root rot, affecting the productivity of numerous horticultural crops [1–3]. The hyphal anastomosis reactions determine the classification of the phytopathogenic fungus *R. solani* into distinct anastomosis groups (AGs) [4]. *R. solani* exhibit variability in terms of their host specificity and virulence levels toward their plant hosts ability to infect specific hosts and the extent of harm they cause to their plant hosts. Conversely, the pathogen *S. rolfsii* has the ability to infect around 500 plant species and is responsible for the substantial decrease in global crop yield. *S. rolfsii* is globally distributed, with a higher prevalence in tropical and subtropical regions [5].

Managing these pathogens can be challenging because of their capacity for infecting different hosts and their capacity to persist for extended durations on plant debris and organic substance in the soil. Even if a host plant is not present, these fungi have the ability to exist either as free-living entities or develop resilient structures such as oospores, microsclerotia, sclerotia, or chlamydospores [6]. The increasing variety of crops in agriculture highlights the need for concurrent expansion of tactics and the development of innovative approaches to effectively manage soil-borne plant diseases. Chemical fungicides have been periodically applied during the cropping season to reduce the occurrence of soil-borne diseases. Nevertheless, the widespread utilization of fungicides results in the disturbance of ecological system, posing health risks to human and animal, together with beneficial species in the soil [7]. The increasing environmental limitations and inadequate management alternatives underscore the necessity for an alternative, sustainable, and efficient management approach. Consequently, there is a substantial focus on the study of environmentally safe and sustainable antifungal agents, including essential oils derived from plants.

Over the past ten years, plant essential oils (EOs), widely recognized for their safety, have been shown to have a wide range of fungicidal potential toward several fungal pathogens. As a result, they have been regarded as biodegradable safe natural alternatives [8,9]. Clove essential oil (CEO), among the EOs, has proven its high potential as a valuable sources of many compounds possessing various biological activities that make its use beneficial in antibacterial and antimicrobial preparation, the food industry, and pesticides manufacturing [10,11]. However, volatile oils face great challenges in their ability to be utilized and absorbed owing to their poor water solubility, and physical and chemical instability [12]. Therefore, nanoemulsions are recognized as a favorable method for encapsulating volatile oils, providing efficient delivery systems that facilitate their practical application in agriculture, food, cosmetics, and pharmaceuticals [13–15].

In the last years, along with the world trend for sustainability, nanoemulsions have emerged as a promising tool for sustainable agriculture and biosafety. Nanoemulsion-based pesticide formulations are colloidal and comprise particles that are exceedingly small, typically falling within the 20–200 nm range. Commonly composed of oil-in-water (O/W type) phases, these emulsions are economically more cost-effective [16,17]. These formulations are designed to effectively mitigate and regulate the effects of

pests and diseases on crops. In agricultural contexts, they have been specifically designed to enhance efficacy by serving as a carrier for the transportation and administration of bioactive compounds to the intended pests [17]. Their high-water solubility enables them to dissolve hydrophilic and lipophilic compounds with ease, which is a significant factor in their cost-effectiveness. As a result, the quantity of inert material and AIs required is being reduced. Enhanced efficacy against pathogenic organisms, including bacteria, fungi, and insects, is a result of the improved solubility and assimilation of these formulations [17,18]. In addition, nanoemulsions exhibit exceptional storage stability across a broad temperature range (−10°C to 55°C). Their efficacy in controlling a variety of storage pests, has been demonstrated [16]). Particularly in the context of pest control, nanoemulsions offer a promising alternative that can enhance the safety of human health and the environment while causing the least amount of damage to non-targeted organisms and the environment [19,20]. Further investigation is necessary to gain a comprehensive understanding of the potential ecological hazards of nanoemulsions and their effects on non-target organisms [21].

Nano-encapsulation has emerged as a more effective method of preserving essential oils (EOs) against oxidation and evaporation [22–24]. It also provides regulated release of encapsulated compounds for extended periods of time [25], enhancing the stability, solubility in water, and bioavailability of lipophilic compounds [26]. Recent research has demonstrated the benefits of employing encapsulated EOs compared to their non-encapsulated counterparts. The evidence substantiates the clear advantages of employing encapsulation techniques, as they shield these bioproducts from environmental factors (e.g., light, humidity, heat, and oxygen), enhance stability, diminish volatility, thereby extending their shelf life, and enable controlled release, which prolongs the compounds' biological impact [27]. Recently, chitosan (CS) has arisen as an issue of considerable interest for encapsulating bioactive chemicals and essential oils, owing to its biocompatibility, biodegradability, nontoxicity, and antibacterial qualities, as well as its capacity for forming particles, films, and gels [24,25,28,29]. Although nano-capsules offer a multitude of benefits, they also pose specific potential obstacles. Their biological impact is also influenced by their unique physicochemical characteristics, which may also present unforeseen noxious hazards. The safe utilization of nanoparticles necessitates a comprehensive understanding of their toxicity [30].

In this context, the current study aims to develop both: a) aqueous phase clove essential oil nanoemulsion (CEONE) utilizing only tween 80 as a surfactant, and b) chitosan/clove nanoemulsion (CS/CEONE), in which clove oil nanodroplets are dispersed homogenously and uniformly with the aqueous solution of chitosan. Afterwards, both nanoemulsions were thoroughly characterized to examine their morphological and physico-chemical properties. The current study also aimed to investigate the inhibitory effects of CEONE and CS/CEONE on the biomass of *R. solani* and *S. rolfsii* through laboratory trial and on stem canker and black scarf diseases caused by *R. solani* as well as to pre-emergence and post-emergence damping-off caused by *S. rolfsii* under greenhouse conditions with a direct comparison with the recommended fungicide.

2 Materials and Methods

2.1 Materials

Chitosan (low molecular weight), tween 80, and glacial acetic acid (reagent grade, ≥99%) were acquired from Sigma Aldrich, Germany. Clove oil (50-mL, purity 100%) was purchased from Nefertari, Egypt.

2.2 Preparation of the Nanoemulsions

2.2.1 Formulation of Primary Emulsions

Clove essential oil-in-water (O/W) nanoemulsion was formulated depending on a previously documented protocol with slight modifications [31]. In brief, emulsification of clove essential oil (CEO) in the aqueous phase was carried out in 1:2 ratios, where the aqueous phase contained tween 80 as a nonionic surfactant. First, the aqueous phase was positioned on a magnetic stirrer at room temperature

(25°C) and humidity of 35%, subsequently supplemented with gradual droplets of CEO to prepare crude emulsion. Afterward, the coarse emulsion underwent additional homogenization utilizing a homogenizer (Daihan, Korea) at 20,000 rpm for 15 min at room temperature (25°C) and humidity of 35% to convert the coarse emulsion into microemulsion through oil droplet size reduction. This is considered to be the primary stage for CEONE. Likewise, the main stage of preparing CS/CEONE was successfully prepared following similar steps. In contrast, the aqueous phase consisted of 0.1% chitosan solution formulated in 1% glacial acetic acid. Additionally, the formulation incorporated tween 80 as the nonionic surfactant at a concentration of 2% w/v.

2.2.2 Formulation of Nanoemulsions

Both pre-formulated microemulsions underwent sonication using a probe sonicator (Model LC 60/H, Elma, Germany) with a sonication probe of 12 mm diameter. The experiment was carried out at room temperature (25°C) and humidity of 35%. The sonication process was carried out using high-power ultrasonic irradiation at 400 W power and 20 kHz. To preserve the stability of the nanoformulations, an ice bath was utilized to immerse the samples during the sonication process to prevent overheating. Sonication was performed for a total of 15 min, with a cycle of 10 s of sonication followed by 5 s of rest, resulting in the formation of the respective nanoemulsion for each sample nanoemulsion [32]. Finally, both CEONE and CS/CEONE nanoemulsions were placed in a refrigerator at 4°C for additional characterization.

2.3 Characterization of the Nanoemulsions

2.3.1 Nanodroplets Size, Polydispersity Index (PDI) and Surface Charge

The Malvern Zeta Sizer (Malvern Panalytical Ltd., Malvern, UK) was used in conjunction with the dynamic light scattering (DLS) method to determine the polydispersity index (PDI), size, distribution and surface charge of the nanodroplets in both CEONE and CS/CEONE nanoemulsions.

2.3.2 Morphological Examination

The size and morphology of both CEONE and CS/CEONE, was microscopically examined with Transmission Electron Microscope (TEM, Jeol, Peabody, MA, USA), where deionized water was employed for dilution. Afterwards, a minute droplet was positioned over a copper grid to be investigated after being stained with phosphotungstic acid.

2.3.3 Physical Characterization and Stability Assessments

Both pH and conductivity of each of the prepared nanoemulsions were estimated at the temperature of the room utilizing a pH and conductivity meter (Jenway, UK). The measurements were performed in triplicate. Both CEONE and CS/CEONE nanoemulsions were assessed for their stability over a 4-week duration. To investigate the nanoformulation's stability, their nanodroplets size, PDI, surface charge, pH and conductivity were checked at different time intervals during the experiment.

2.3.4 Chemical Characterization

Fourier Transform Infrared Spectroscopy (FTIR)

To study the chemical composition of both CEONE and CS/CEONE nanoemulsions, FTIR (Thermo Scientific, Waltham, MA, USA) was employed. This involved studying the chemical structures of the individual components of both nanoemulsions within the range of 400–4000 cm^{-1}. Hence, the chemical structure of clove oil, tween 80, and chitosan was investigated individually in addition to both CEONE and CS/CEONE nanoformulations.

Ultraviolet Visible Spectroscopy (UV-Vis)

To investigate the effect of the used protocols and purity of the used materials on the chemical structure of clove oil, UV-Vis spectroscopy was followed. Therefore, pure clove oil as well as clove oil extracted from both CEONE and CS/CEONE nanoemulsions were scanned using UV-Vis spectroscopy. The wavelength of maximum absorbance was determined for the three samples as an indication of the purity and preservation of the chemical structure of clove oil after being incorporated in different NE systems [33].

2.4 In Vitro Release and Kinetic Profile

To determine the release behavior of clove oil from both nanoemulsion systems, a pre-prepared drug release setup was utilized, wherein 1 mL of each nanoemulsion was singly placed [34]. The cumulative release of clove oil, the dialysis bag method technique has been followed. In a nutshell, a receptor medium consisting of a buffer solution (pH 5.5) containing a 0.1% aqueous solution of tween 80 was employed to replicate the actual oil release environment during its application. The entire experimental setup for release was kept in a shaking incubator during the whole duration of the experiment at 37°C and 60 rpm. Afterwards, an amount of 2 mL sample of the receptor medium of each sample was withdrawn individually and substituted by an equivalent amount of fresh buffer. The clove oil concentrations within the collected samples were determined utilizing a UV-Vis spectrophotometer (Thermoscientific, USA) at 283 nm wavelengths. Ultimately, the cumulative release pattern of clove oil was computed for the two nanoemulsion systems. The cumulative release experiment was conducted in triplicate.

2.5 The Tested Fungi

The two fungal pathogens *Sclerotium rolfsii* Sacc. and *Rhizoctonia solani* J.G. Kuhn were isolated from diseased stems and roots of potato plants. The cultures were preserved on potato dextrose agar (PDA) medium at 4 ± 2°C till use. The identification of both fungi was initially done by examining colony morphology and microscopic examination of mycelium. Molecular characterization was carried out to confirm their identity after DNA extraction from fresh mycelium employing the Dellaporta DNA isolation protocol [35]. The internal transcribed spacer region (ITS) of rRNA was sequenced and amplified using primer pairs ITS4 and ITS5 [36]. PCR amplification was performed in a 2720 Thermal Cycler (Applied Biosystems, Foster City, California) following a previously reported protocol [37]. The PCR products obtained underwent cleaning and sequencing in both forward and reverse directions, utilizing the sequencing service provided by Macrogene Inc. (Seoul, Korea). Then, the sequences underwent editing and were curated as necessary using MEGA 11 software [38]. The sequence homology was assessed utilizing BLAST® *vs.* the sequence database of NCBI (National Center for Biotechnology Information, GenBank; www.ncbi.nlm.nih.gov/genbank, accessed on 15 August 2024).

2.6 Pathogenicity Test of Isolated Fungi

2.6.1 Inoculum Preparation

In sterilized glass flasks (500 mL), the inoculum of the tested *R. solani* and *S. rolfsii* was prepared. Each flask held a blend of sorghum grains and sand in a 2:1 volume ratio. The components were thoroughly mixed, moistened with tap water, and then autoclaved at 121°C for 30 min. The flasks were inoculated with a 6 mm mycelial disc from a 5-day-old culture of each fungus. Then, the inoculated flasks were incubated at 24 ± 2°C for 15 days [39].

2.6.2 Soil Mixture and Inoculation

A soil mixture of peat moss and sand (2:1 w/w) was prepared and sterilized using a 5% diluted solution of commercial formalin. Plastic pots measuring 30 cm in diameter were sterilized by immersing them in a 5% formalin solution for 15 min, followed by air drying for 24 h. Subsequently, the pots were occupied with 3 kg of the pre-prepared sterilized soil mixture. Each pot was then inoculated with the inoculum at a rate of 2% and

irrigated for 5 days pre-planting [39]. The control pots were treated with the autoclaved sorghum-sand mixture devoid of fungi. Potato tubers of the cv. Spunta were planted in plastic pots (one tuber per pot) and were fertilized and watered as necessary. Each pair of pots constituted a single replicate, with three replicates allocated to each treatment. The pots were maintained under greenhouse conditions.

2.6.3 Disease Assessment

Disease Severity (DS) of stem canker were assessed after 90 days of planting employing the scale of Carling et al. [40] as following: 0 = no damage or lesions present, 1 = one to several lesions less than 5 mm in size, 2 = lesions larger than 5 mm and some girdling present, 3 = large lesions and girdling or death on most stems, 4 = all stems killed.

Whereas DS of black black scurf was assessed using the scale of Hadi et al. [41] as following: 0 = no sclerotia present, 1 = less than 1% of the tuber surface area covered in sclerotia, 2 = 1% to 10%, 3 = 11% to 20%, 4 = 21% to 50% and 5 = 51% or more.

Disease Severity was calculated using the following equation:

$$(\mathrm{DS})\% = \sum (\text{No. of infected tubers} \times \text{No. of scale}) \ \text{Total No. of tubers} \times \text{highest No. of scale} \times 100.$$

The disease incidence was determined as follows:

$$\text{Disease Incidence}(\mathrm{DI})\% = \text{No. of infected tubers}/\text{Total No. of tubers} \times 100.$$

The pre-emergence and post-emergence damping off caused by *S. rolfsii* were calculated following the formula of El-Sayed et al. [42]:

The percentage of pre-emergence damping off was determined after 15 days:

$$\text{Pre} - \text{emergence}\,(\%) = \text{No. of ungerminated sprouted eyes}/\text{Total No. of sprouted eyes} \times 100$$

The percentage of post-emergence damping off was determined after 30 days:

$$\text{Post} - \text{emergence}(\%) = \text{No. of died plants}/\text{Total No. of plants} \times 100$$

2.7 Antifungal Activity of CEO, CEONE, and CS/CEONE against R. solani and S. rolfsii

2.7.1 Laboratory Trial

The antifungal activity of bulk CEO, CEONE, and CS/CEONE toward *S. rolfsii* and *R. solani* was determined on the PDA medium following the previously reported method [43]. They were tested at concentrations of 0.05, 0.1, 0.25, and 0.5, being corresponded to 50, 100, 250, and 500 µL of essential oil, respectively. The concentrations mentioned above were added to the PDA plates. Tween 20, 0.01% (v/v), was introduced to enhance the EO solubility. Plates supplemented with the same volume of tween 20 solution free from EO served as controls. Subsequently, inoculations with *R. solani* or *S. rolfsii* mycelial plugs were performed on each plate, followed by four-day incubation period at 28°C. For each concentration, the experiment was replicated in triplicate, and the antifungal efficacy was assessed by measuring the diameter of the colonies employing the crossover technique. The relative inhibitory rate of mycelial growth, inhibition was computed using the previously described equation [44].

$$\text{Growth inhibition } (\%) = [(R1 - R2)/R1] \times 100$$

where R1 = pathogen's radial growth in the positive control, and R2 = pathogen's radial growth on the treated plate.

2.7.2 Greenhouse Trial

The antifungal activity of CEO, CEONE, and CS/CEONE toward *R. solani* and *S. rolfsii* was evaluated under greenhouse circumstances during the growing season of 2023. Inoculum preparation and inoculation

were carried out for both fungi as described above in the pathogenicity test section. The tested CEO, CEONE, and CS/CEONE were applied by soaking apparently healthy potato tubers cv. Spunta in a series of concentrations (50, 100, 250 and 500 µL/L) for one hour, and Flutolanil 25% was applied at recommended dose of 3 g/kg tubers. Potato tubers used for control were soaked in only sterile water for one hour. Control pots were inoculated with the autoclaved sorghum-sand mixture devoid of fungi. The trials were carried out in a complete randomized block design with three replicates for each treatment. DI and DS of stem canker and black scurf as well as pre- and post-emergence damping-off, were determined as described in the pathogenicity test section. The efficacy of each treatment was calculated using the subsequent equation: Efficacy (%) = Control − Treatment/Control × 100.

2.8 Scanning Electron Microscopy (SEM)

The cytological alternations of hyphae of *R. solani* and *S. rolfsii* due to treatment with CEO NE and CS/CEONE were observed using SEM. Sections of mycelial discs (5 mm) were prepared and mounted on stubs via double-sided adhesive. Subsequently, a coating of gold-palladium was applied to the samples using a sputter coating process. SEM images were captured utilizing JEOL GM 5200 SEM at the Applied Center for Entomonematodes (ACE), Faculty of Agriculture, Cairo University, Giza, Egypt.

2.9 Determination of Extracellular Enzyme Activities

The inhibitory effects of bulk CEO, CEONE and CS/CEONE in decreasing the activity of pectinase and cellulase produced by *R. solani* and *S. rolfsii* were determined. Production of pectinase and cellulase was performed on liquid Czapek's medium containing citrus pectin 5.0 g; Na_2No_3, 2.0 g; KH_2PO_4, 1.0 g; KCl, 0.50 g; $MgSO_4$ $7H_2O$, 0.50 g and $FeSO_4$ 7 H_2O 0.01 g in 1 L of distilled water with 7.2 pH as previously described [45]. The media was autoclaved for 15-min at 121°C. Subsequently, a mycelial plug measuring (1 cm in diameter) from each fungus was inoculated into the flask and incubated for 7-day on an orbital shaker (150 rpm and 28–30°C). Each treatment, including the control, was replicated in 3 times as the entire experiment. The mycelial matt was removed from the broth culture in each flask through filtration followed by 15-min centrifugation at 4000 g at 4°C. Subsequently, the supernatants obtained were utilized for the preparation of crude enzymes.

2.9.1 Pectinase Activity

Pectinase activity was assessed following the previously reported procedure [46]. The reaction mixture, consisting of diluted crude enzyme and 1% pectin prepared in sodium acetate buffer (0.05 M; pH 5.5), and incubated for 30-min in water bath at 50°C. To stop the reaction, the supplementation of 1.0 ml of a dinitrosalicylic acid was added, followed by 10-min boiling of the mixture then cooling [46]. The activity was assessed spectrophotometrically at 540 nm and 30°C. Using a standard glucose solution, a standard graph was created. The activity of pectinase was quantified as one unit, representing the quantity of enzyme that released 1 µm of glucose per minute.

2.9.2 Cellulase Activity

Cellulase activity was assessed following the previously reported procedure [46]. The reaction mixture comprised 1 mL of the supernatant and 1 mL of 0.5% pure cellulose (Sigma Co.) suspended in 50 mM phosphate buffer (pH 5.0). The mixture was incubated for 30 min at 50°C. Blanks were prepared by replacing the supernatant with distilled water. Absorbance was determined spectrophotometrically at 540 nm. One unit of cellulase activity was defined as the quantity of enzyme that released 1 µmol of glucose per minute.

2.10 Statistical Analyses

The data were analyzed using one-way analysis of variance (ANOVA) based on Snedecor and Cochran statistical method [47] and means were compared utilizing the Least Significant Difference analysis test

(LSD) at the level of $p < 0.05$. Statistical analysis was conducted with SPSS (Statistics for Windows, Version 21.0, USA) software.

3 Results

3.1 Nanodroplets Size, Polydispersity Index (PDI) and Surface Charge

Data in Table S1 inferred that CEONE possesses a larger size (86 ± 3 nm) and a broader PDI range (0.121 ± 0.011) compared to CS/CEONE. While CS/CEONE possess a smaller size of 49 ± 4 nm and narrower PDI of 0.099 ± 0.009. Interestingly, both NE formulations exhibit an optimal size, ensuring their high stability. Furthermore, results of zeta potential demonstrated that both CEONE and CS/CEONE exhibit surface-charged droplet exceeding −20 and +27 mV, respectively. Moreover, CS/CEONE exhibits a higher surface charge than CEONE.

3.2 Physical Characterization

Both CEONE and CS/CEONE were investigated for their physical characteristics concerning pH and conductivity as revealed from the results presented (Table S1). It was observed that both nanoemulsions exhibited an acidic nature, possessing pH values of 5.60 and 5.03, respectively. This denotes that the followed preparation protocol was successfully carried out without altering the acidic nature of the used clove oil.

3.3 Stability Assessments

Both CEONE and CS/CEONE systems were monitored for their stability along a 4-week duration in terms of surface charge, PDI, size, pH and conductivity (Table S2). The results revealed that both NE systems kept their size and PDI values almost constant within the first week. However, CEONE nanodroplets size started to show a slight gradual increase in both size and PDI with increasing time indicating corresponding slight coalescence of the oily nanodroplets. On the other hand, CS/CEONE nanodroplets showed a very minute increase in size compared to CEONE. Finally, it has been found that there was no significant distinction in both pH and conductivity values for both NE systems along the 4-week duration which confirms the preservation of the nanoformulations properties and structures without any noticeable changes.

3.4 Morphological Characterization

TEM investigation revealed that both CEONE and CS/CEONE exhibited uniform spherical nanodroplets (Fig. 1a,b), respectively. Moreover, the results from TEM image analysis are found to align with those obtained from zeta sizer, where CS/CEONE displayed smaller spherical nanodroplets with a narrower size distribution (PDI) than CEONE. CEONE and CS/CEONE showed nanodroplets of 71 ± 5 nm and 32 ± 6 nm, respectively (Fig. 1a,b). It is found that size obtained from both TEM and zeta sizer measurements are quite near. However, size results obtained from zeta sizer are slightly larger compared to their corresponding results obtained from TEM imaging.

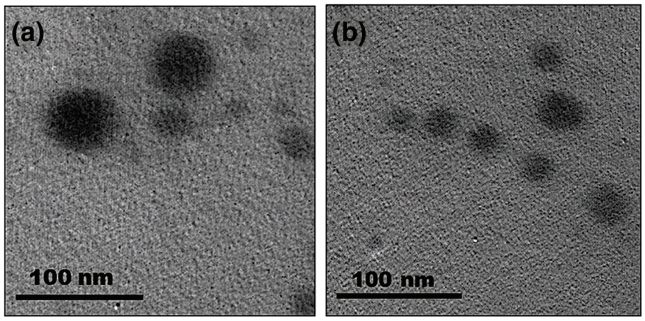

Figure 1: TEM Imaging of CEONE (a) and CS/CEONE (b) systems

3.5 Chemical Characterization

3.5.1 Fourier Transform Infrared Spectroscopy (FTIR)

Both CEONE and CS/CEONE systems have been studied using FTIR spectroscopy of the chemical structure of each component as well as the final nanoformulations (Fig. 2a). Pure clove oil (CO) spectrum shows distinctive bands at 3709 and 1939 cm^{-1}, indicating O-H and C-O stretching, respectively. Furthermore, pure chitosan (CS) spectrum exhibits a characteristic broad peak at 3606 cm^{-1}, indicating the stretching of NH_2 and O-H groups. Both the abundance of the C = O bond within the $NHCOCH_3$ group, represented by the amide I band, and the existence of N-H bending and C-O stretching, indicated by the amide II band, were determined through observing the distinct peak at 1609 cm^{-1}. It is observed that CEO and CEONE are superimposable and totally identical. This confirms that the preparation method employed for CEONE had no effect or change the chemical structure on CEO. Finally, the appearance of the distinctive peaks of both CEO and CS within the spectrum of CS/CEONE assures the successful incorporation of both CS and CEO within the nanoemulsion system. Moreover, the decrease in the intensity of peaks characteristic of CEO within CS/CEONE system proves the successful formation of shell surrounding CEO nanodroplets.

3.5.2 UV-Visible Spectroscopy (UV-Vis)

The UV-Vis spectra for pure CEO and CEO extracted from both CEONE and CS/CEONE systems are shown in Fig. 2b. It has been recognized that the three spectra are superimposable and completely identical as shown above. Interestingly, it has been found that all of them show a peak of maximum absorbance at 283 nm. This confirms that the incorporation of CEO in either CEONE or CS/CEONE systems did not alter the chemical composition of CEO emphasizing the convenience of the followed protocol.

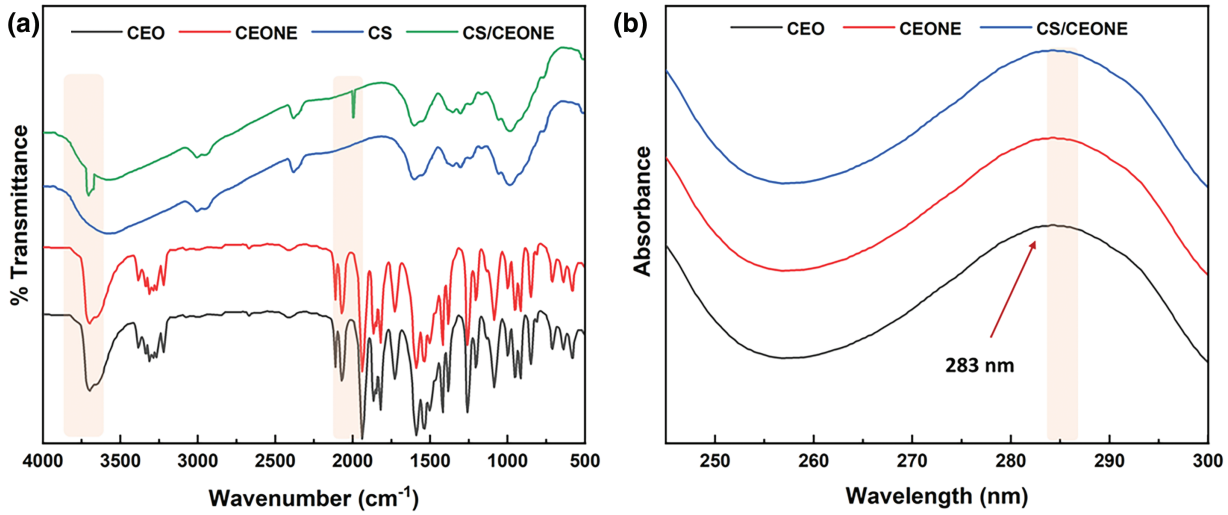

Figure 2: Chemical characterization of CEONE and CS/CEONE systems: (a) FTIR Spectroscopy and (b) UV-Vis Spectroscopy

3.6 In Vitro Release and Kinetic Profile

The concentrations of CEO were estimated at time periods utilizing a UV-Vis spectrophotometer. The cumulative release of CEO from both CEONE and CS/CEONE systems was computed and plotted as shown in Fig. 3. The results in Fig. 3 revealed that CEO was completely released within 12 h from CEONE. However, it has demonstrated a sustained and prolonged release profile from CS/CEONE for up to 4 days. The results show that CS/CEONE, system released around 25% of the initially incorporated

amount of CEO within the first 4 h, and 50% of the quantity in the initial 24 h followed by a continuous controlled release over the 3-day period. This returns back to the abundance of the swell able chitosan shell surrounding the oily nanodroplets.

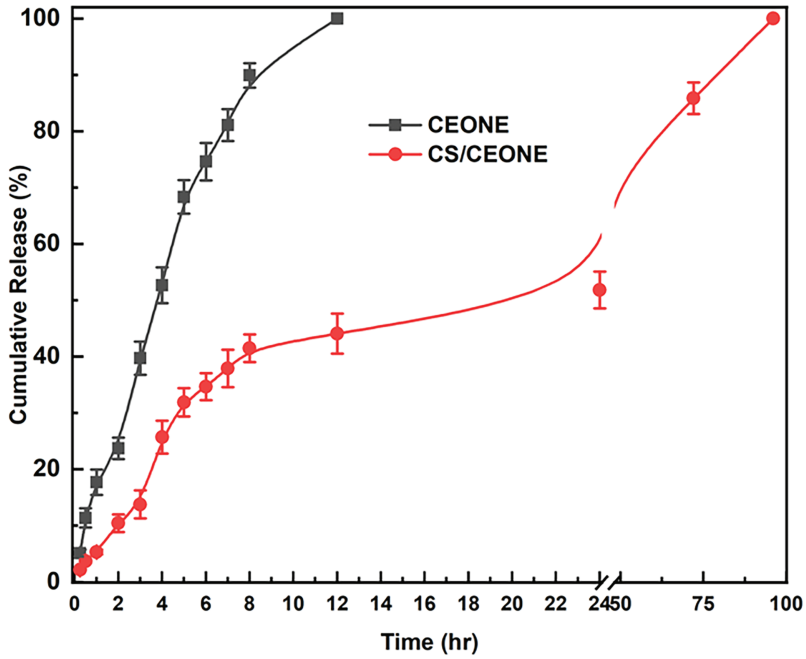

Figure 3: Profile of CEO release from CEONE and CS/CEONE systems

3.7 Characterization of Tested Fungi

S. rolfsii and *R. solani* were recovered from roots of potato and initially tested for pathogenicity and identified based on their mycelial and sclerotial characters described by Ellis [48]. The generated sequences underwent a Blastn search against the GenBank database. According to a megablast search of NCBI's GenBank nucleotide database, closest hits utilizing isolates' ITS sequences of EGY-RS23 exhibited highest similarity 100% to *R. solani* (GenBank Accessions; MK532911, MH259594 and MZ312559). Further, the closest hit utilizing the ITS sequence of the isolate EGY-SR1423 had 100% similarity to *S. rolfsii* (GenBank Accessions; MH854711). The obtained isolates EGY-RS1023 and EGY-SR1423 were assigned accession numbers PQ200681 and PP467723, respectively, upon their deposition in the GenBank database.

3.8 Pathogenicity of Tested Fungi

All tested *R. solani* isolates were capable of inducing stem canker and black scurf on potato stem and tubers, with DI ranging from 53.3% to 90%, and 46.67% to 83.33%, respectively (Table 1). A significant ($p < 0.05$) variation in aggressiveness toward potato was noted among *R. solani* isolates, as reflected in DS varying from 15.06% to 29.49% for black scurf and 20.58% to 35.32% for stem canker. Furthermore, all tested isolates of *S. rolfsii* were pathogenic on potato (Table 2). Pre-emergence damping-off ranged from 50% (by isolates EGY-SR1523, EGY-SR1723 and EGY-SR1823) to 66.7% (by isolate EGY-SR1423). There was a significant ($p < 0.05$) variation in pre-emergence damping-off caused by *S. rolfsii* isolates. However, according to statistical analysis, there was no significant ($p < 0.05$) variation in post-emergence damping-off as well as the total pre-emergence and post-emergence damping-off caused by *S. rolfsii* isolates (Table 2).

Table 1: Stem canker and black scurf diseases caused by *R. solani* on potato

Isolates	Stem canker		Black scurf	
	DI (%)	DS (%)	DI (%)	DS (%)
EGY-RS23	90.0 ± 10a	35.32 ± 2.2a	83.33 ± 5.8a	29.49 ± 1.7a
EGY-RS24	70.0 ± 10b	30.49 ± 1.5b	66.67 ± 5.8b	26.06 ± 1.6b
EGY-RS25	53.3 ± 5.8c	24.39 ± 2.3c	46.67 ± 11.5c	15.06 ± 0.3d
EGY-RS26	90.0 ± 10a	20.58 ± 2.2d	60.00 ± 10b	17.24 ± 0.9d
EGY-RS27	76.7 ± 5.8ab	28.15 ± 0.9b	73.33 ± 11.5ab	20.12 ± 1.9c
Control	0 ± 0d	0.00 ± 0e	0.00 ± 0d	0.00 ± 0e

Note: Values expressed within columns represent the average of three repetitions and means marked with different letters denote significant differences (LSD test, $p < 0.05$). DI = disease incidence; DS = disease severity.

Table 2: Pre-emergence and Post-emergence damping-off caused by *S. rolfsii* on potato

Isolates	Pre-emergence damping-off (%)	Post-emergence damping-off (%)	Pre- and Post-emergence damping-off (%)
EGY-SR1423	66.7 ± 5.8a	20.0 ± 10a	86.7 ± 5.8a
EGY-SR1523	50.0 ± 10b	23.3 ± 5.8a	73.3 ± 5.8ab
EGY-SR1623	60.0 ± 10ab	20.0 ± 10a	80.0 ± 10ab
EGY-SR1723	50.0± 10b	16.7 ± 5.8a	66.7 ± 5.8b
EGY-SR1823	50.0 ± 10b	23.3 ± 5.8a	73.3 ± 11.5ab
Control	0.0 ± 0c	0.0 ± 0b	0.0 ± 0c

Note: Values expressed within columns represent the average of three repetitions and means marked with different letters denote significant differences (LSD test, $p < 0.05$).

3.9 Antifungal Activity of CEO, CEONE and CS/CEONE against Mycelial Growth and Biomass of R. solani and S. rolfsii

It is evident from the Fig. 4a,b that CEO, CEONE, and CS/CEONE have shown significant antifungal activity by hindering the mycelial growth of *R. solani* and *S. rolfsii* across all tested concentrations. Following 24 h of incubation, no visual growth was observed for both fungi on PDA medium supplemented, with CEONE and CS/CEONE at the higher concentrations of 250 and 500 µL/L. The greatest growth inhibition against *R. solani* was maintained with utilizing CEONE and CS/CEONE at concentration 500 µL/L, with significant ($p < 0.05$) variation among them with value ranging from 56.11% to 71.94% and 52.2% to 79.2%, respectively. Similar results were also noticed for *S. rolfsii*, of which CS/CEONE followed by CEONE gave the highest inhibitory effect against *S. rolfsii* after 96 h. with value reached 50.6% and 44.1%, respectively. Whereas, the minimum inhibition against these pathogens was noticed for CEO at all concentrations with inhibition value ranging from 43.33% to 55.83% for *R. solani* and 21.6% to 37.7% for *S. rolfsii*. The inhibitory effect of CEONE and CS/CEONE showed dose-dependent activity against mycelial growth of both fungi. Fresh mycelial biomass of *S. rolfsii* and *R. solani* were significantly ($p < 0.05$) decreased in liquid medium treated with the CEO, CEONE and CS/CEONE at all tested concentrations (Fig. 5b). In general, it may be stated that CS/CEONE significantly decreased the total biomass of *R. solani* to value reached 1.14 g, with efficacy up to 78.45% (Fig. 5a). While the same treatment decreased the fungal biomass of *S. rolfsii* to value reached 1.48 g, with efficacy 73.87% (Fig. 5b).

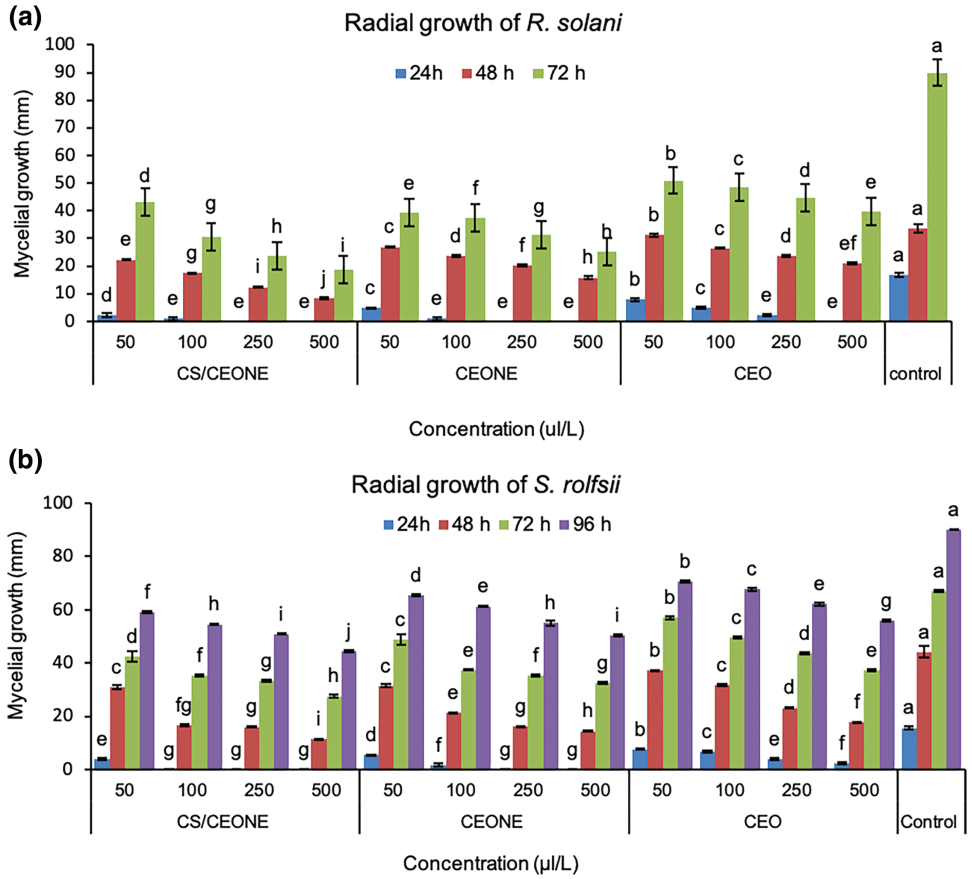

Figure 4: Mycelial growth (mm) of *R. solani* (a) and *S. rolfsii* (b) at different concentrations of CEO, CEONE, and CS/CEONE. The values indicated inside columns are the mean of three replicates ± standard deviation. Bars highlighted by distinct letters differ considerably ($p < 0.05$), as demonstrated by the LSD test

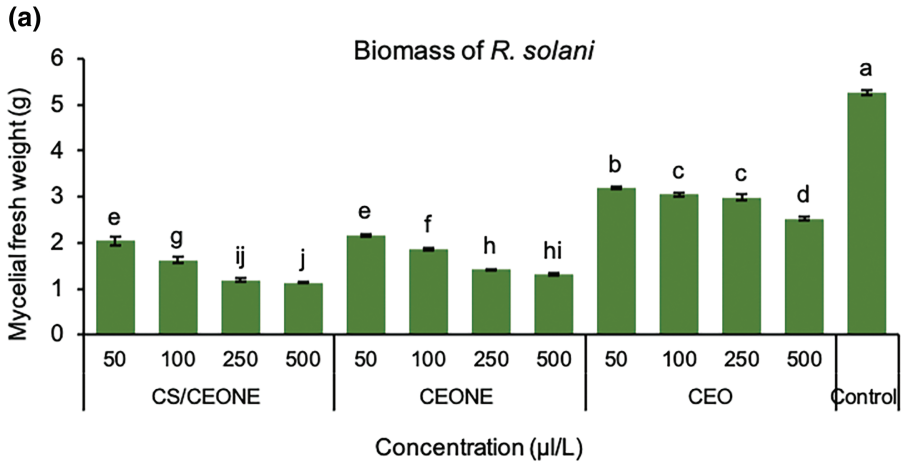

Figure 5: (Continued)

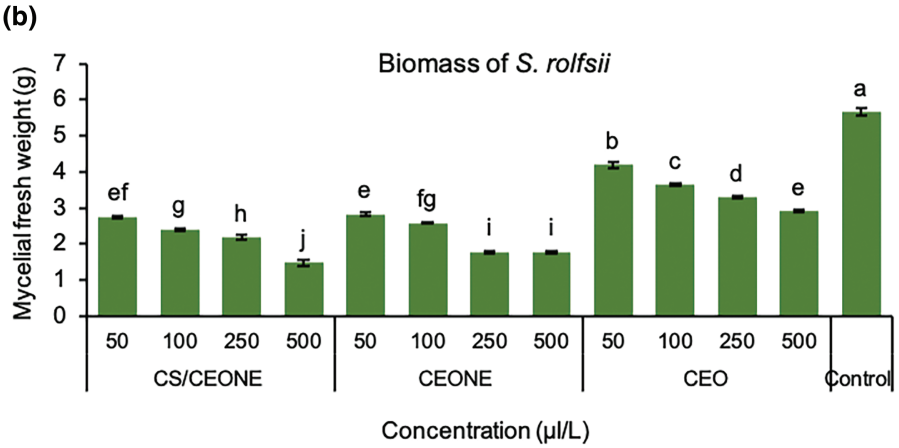

Figure 5: Mycelial fresh weight (gm) of *R. solani* (a) and *S. rolfsii* (b) grown in PDA media treated with CEO, CEONE, CS/CEONE, and untreated (control). The values indicated inside columns are the means of three replicates ± standard deviation. Bars highlighted by distinct letters differ considerably ($p < 0.05$), as demonstrated by the LSD test

3.10 Effect of the CEO, CEONE, and CS/CEONE on Enzymatic Activity of R. solani and S. rolfsii

Results in Fig. 6a revealed that CEO, CEONE and CS/CEONE at all tested concentrations were efficient in decreasing the effect of pectinase and cellulase produced by the tested fungi. In this regard, activity of cellulase produced by *R. solani* was significantly ($p < 0.05$) decresed in the occurrence of CS/CEONE and CEONE at highest concentrations of 500 µL/L, which recorded 0.012 and 0.015 U/mL, respectively. Pectinase enzyme secreted by *R. solani* was also decreased in the presence of CS/CEONE and CEONE at concentration of 500 µL/L, which registered 0.007 and 0.014 U/mL, respectively. CEO was also effective in diminshing the activity of cellulase and pectinase released by *R. solani* to values reached 0.038 and 0.033 U/mL, respectively, with reduction percentage of 58.24% for cellulase and 79.79% for pectinase. In overall, treatment of CS/CEONE at concentration of 500 µL/L revealed the most significant decrease in the cellulase and pectinase activities for *R. solani* with values reached 86.94% and 93.69%, respectively.

Activity of pectinase and cellulase secreted by *S. rolfsii* was also negatively impacted by CEO, CEONE and CS/CEONE treatments at all tested concentrations (Fig. 6b). Cellulase activity was very low in CEONE-treated media at concentration 500 µL/L and reached 0.050 U/mL, with reduction percentage of 87.05%. Furthermore, treatment of CS/CEONE at the same concentration significantaly ($p < 0.05$) decresed the activity of cellulase secreted by *S. rolfsii* to reach 0.076 U/mL, with decresed percentage of 78.44%. In contrast to this result, CEO was the least effective in decreasing the cellulase activity, which recorded 0.132 U/mL. Moreover, treatments with CEO, CEONE and CS/CEONE at concentration 500 µL/L negatively influenced the production of pectinase enzyme to values reached 0.165, 0.049, and 0.080, respectively. Overall, the most substantial decrease in pectinase activities of *S. rolfsii* was recognized utilizing the CS/CEONE followed by CEONE.

3.11 Scanning Electron Microscopy (SEM)

SEM observations of vegetative growth of *R. solani* (Fig. 7) and *S. rolfsii* (Fig. 8) on PDA supplemented with the CEONE and CS/CEONE showed degenerative changes in hyphal morphology. SEM images show morphological alteration, crinkling, distortion, and spoiling the hyphae of *R. solani* and *S. rolfsii* because of CEONE and CS/CEONE compared to the hyphae of untreated control. At higher concentrations of 250 and 500 µL/L, cell wall disruptions (arrows) along with subsequent hyphal lysis or necrosis were noticed

(Figs. 7c,d and 8c,d). In both investigated fungi, the control mycelium cultured on PDA exhibited a normal morphology (Figs. 7 and 8).

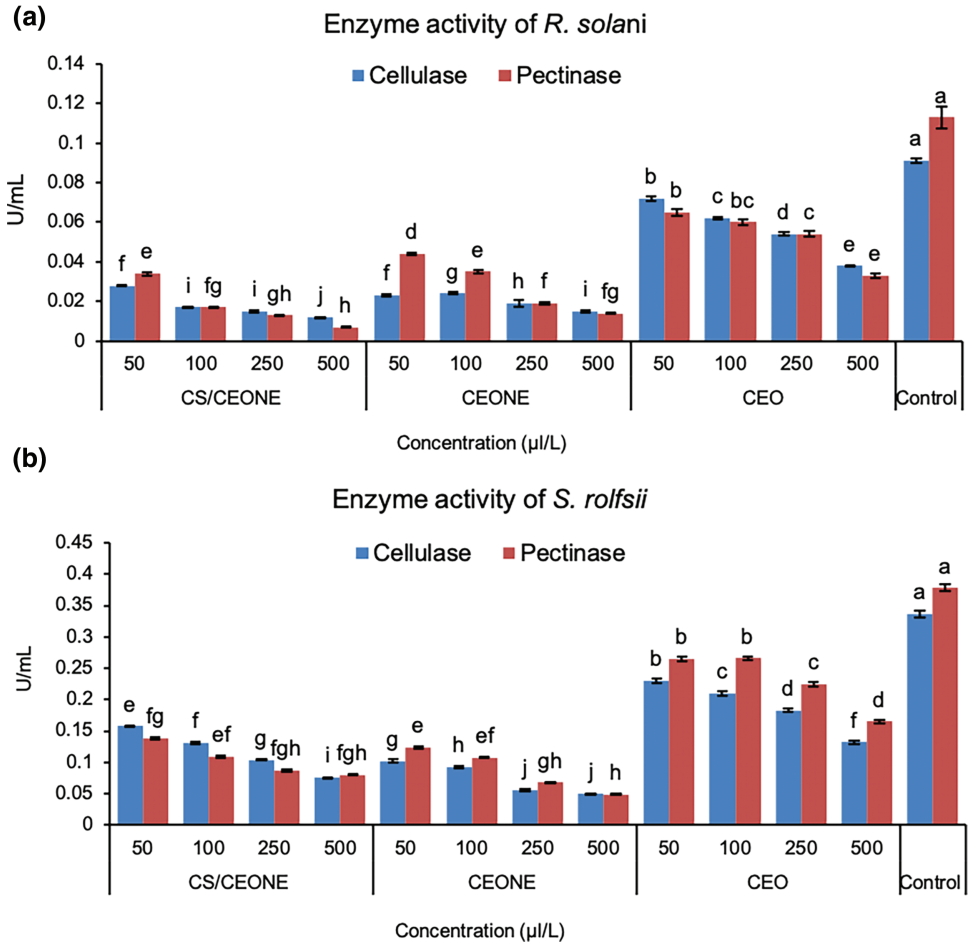

Figure 6: Enzymatic activity of cellulase and pectinase of *R. solani* (a) and *S. rolfsii* (b) in liquid Czapek's media treated with CEO, CEONE, CS/CEONE, and untreated (control). The values indicated below columns are the means of three replicates ± standard deviation. Bars highlighted by distinct letters differ considerably ($p < 0.05$), as demonstrated by the LSD test

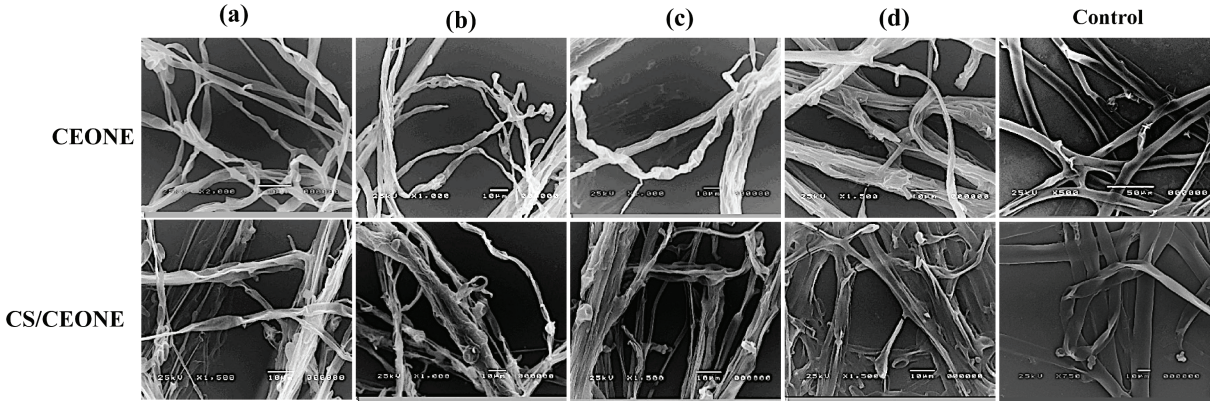

Figure 7: Scanning electron microscope (SEM) images of hyphal morphology of *R. solani* after 72 h. on PDA medium amended with CEONE and CS/CEONE at concentrations 50 (a), 100 (b), 250 (c) and 500 µL/L (d), and control

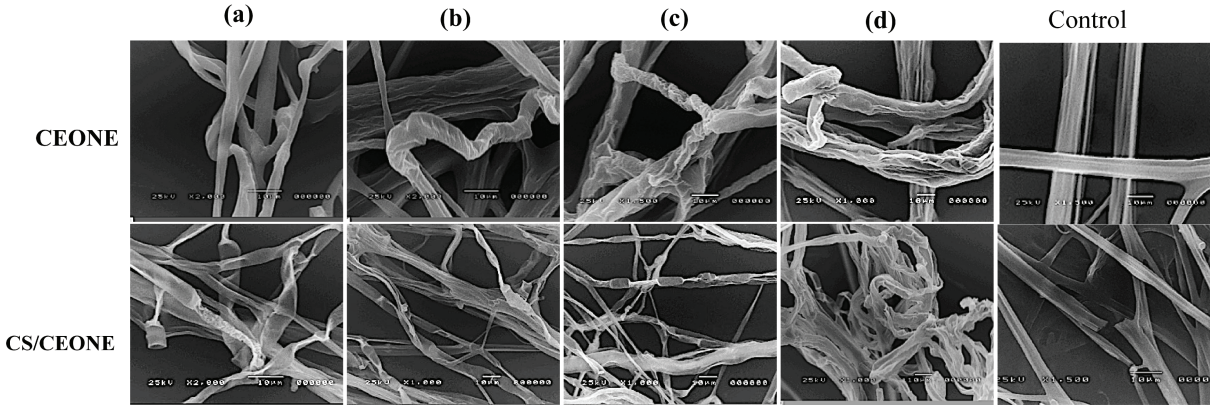

Figure 8: Scanning electron microscope (SEM) images of hyphal morphology of *S. rolfsii* after 96 h. on PDA medium supplemented with CEONE and CS/CEONE at concentrations 50 (a), 100 (b), 250 (c) and 500 µL/L (d), and control

3.12 Antifungal Activity of CEO, CEONE and CS/CEONE against R. solani and S. rolfsii under Greenhouse Conditions

The data presented in Table 3 shows that the tested CEO, CEONE, and CS/CEONE at all concentrations significantly ($p < 0.05$) decreased DI% and DS% of black scurf and stem canker diseases in greenhouse conditions compared to the control. The greatest effect was acquired by CS/CEONE at 500 µL/L, which showed a significant decrease in DI% and DS% with efficacy reached 77.78% and 71.7% for stem canker and 83.33% and 75.12% for black scurf (Table 3). A similar trend of findings was also noted for CEONE, which recorded a significant ($p < 0.05$) reduction in DI% and DS% at 500 µL/L, with efficacy reached 77.78 and 57.12 for stem canker and 75% and 69% for black scurf. In *S. rolfsii* trial, the same trend was obtained, of which the higher concentration (500 µL/L) of each of CEONE and CS/CEONE had the highest effect in decreasing DI and DS of pre-emergence and post-emergence damping-off symptoms (Table 4). Increasing the concentrations of the tested compounds (CEO, CEONE, and CS/CEONE) from 50 to 500 µL/L gradually increased their effectiveness in reducing the DI% and DS% of black scurf, stem canker, pre-emergence damping-off, and post-emergence damping-off diseases on potato. According to statistical analysis, no significant ($p < 0.05$) distinctions noted between the treament with Flutolanil 25% and CEONE or CS/CEONE in reducing pre-emergence and post-emergence damping-off symptoms (Table 4). Non-phytotoxic effects were observed on potato leaves in response to the evaluated treatments throughout the trial studies.

Table 3: Evaluation of CEO, CEONE, and CS/CEONE against stem canker and black scurf of potato caused by *R. solani*

Treatments	Conc. (µL/L)	Stem canker				Black scurf			
		DI (%)	Effic. (%)	DS (%)	Effic. (%)	DI (%)	Effic. (%)	DS (%)	Effic. (%)
CEO	50	83.33 ± 5.77a	7.4	31.19 ± 1.62b	11.88	66.67 ± 5.77b	16.67	25.64 ± 1.29b	11.59
	100	80.0 ± 10a	11.11	29.18 ± 1.11c	17.55	53.33 ± 11.55cd	33.33	24.01 ± 1.31b	17.21
	250	60 ± 10b	33.33	27.26 ± 0.63c	22.02	56.67 ± 5.77bc	29.17	20.85 ± 203c	28.11
	500	56.67 ± b	37.04	25.26 ± 1.02d	28.62	46.67 ± 5.77cde	41.67	19.17 ± 1.06c	33.89
CEONE	50	60.0 ± 10b	33.33	21.51 ± 1.38b	39.23	53 ± 5.77b	33.33	16.33 ± 1.5b	43.7
	100	53.33 ±11.55b	40.74	20.21 ± 1.96bc	42.89	50 ± 10b	37.5	12.98 ± 1.8c	55.25

(Continued)

Table 3 (continued)

Treatments	Conc. (µL/L)	Stem canker				Black scurf			
		DI (%)	Effic. (%)	DS (%)	Effic. (%)	DI (%)	Effic. (%)	DS (%)	Effic. (%)
	250	26.67 ± 5.77c	70.37	16.13 ± 1.01d	54.41	23 ± 5.77d	70.83	9.06 ± 1.06e	68.75
	500	20.0 ± 10c	77.78	15.18 ± 0.73d	57.12	20 ± 10de	75	8.99 ± 1.04e	69.01
CS/CEO NE	50	50.0 ± 10b	44.44	18.51 ± 1.07c	47.69	43 ± 5.77bc	45.83	13.93 ± 13.93c	51.97
	100	46.67 ± 11.55b	48.15	12.41 ± 0.72e	64.93	37 ± 5.77c	54.16	11.25 ± 0.96d	61.19
	250	23.33 ± 5.77c	74.075	10.61 ± 1.0ef	70.01	13 ± 5.77de	83.33	7.39 ± 1.5f	74.52
	500	20.00 ± 10c	77.78	10.02 ± 0.86f	71.7	13 ± 5.77de	83.33	7.21 ± 0.85f	75.12
Flutolanil 25%		13.33 ± 5.77cd	85.19	7.0 ± 20.68g	78.96	10 ± 10ef	87.5	3.73 ± 0.66g	87.14
Infected control		90.00 ± 10a	0	35.39 ± 2a	0	80 ± 10a	0	29.0 ± 1.7a	0
Healthy control		0.00 ± 0a		0.0 ± h	0.00	0 ± 0f	100	0 ± 0h	100
LSD		15.14		1.92	21.51	12.96		1.42	

Note: Values expressed within columns represent the average of three repetitions and means marked with different letters denote significant differences (LSD test, $p < 0.05$). Effic. = efficacy; DI = disease incidence; DS = disease severity; Conc. = concentration.

Table 4: Evaluation of CEO, CEONE, and CS/CEONE against pre-emergence and post-emeregence damping-off on potato caused by *S. rolfsii*

Treatments	Conc. (µL/L)	Pre-emergence damping-off (%)	Effic. (%)	Post-emergence damping-off (%)	Effic. (%)	Pre+Post-emergence damping-off (%)	Effic. (%)
CEO	50	63.33 ± 5.77ab	5	23.33 ± 5.77a	0	86.67 ± 5.77ab	3.7
	100	60 ± 10abc	10	23.33 ± 5.77a	0	83.33 ± 11.55ab	7.14
	250	53.33 ± 5.77bcd	20	20 ± 10ab	14.27	73.33 ± 15.28cd	18.52
	500	46.67 ± 5.77de	30	13.33 ± 5.77abc	42.85	60.00 ± 10.0 de	33.33
CEONE	50	56.67 ± 5.77ab	15	20 ± 10ab	14.27	76.67 ± 5.77bc	14.8
	100	46.67 ± 5.77bc	30	20 ± 10ab	14.27	66.67 ± 11.55cd	25.93
	250	36.67 ± 5.77cd	45	10 ± bcd	57.14	46.67 ± 11.55fg	48.15
	500	26.67 ± 5.77de	60	6.67 ± 5.77cd	71.42	33.33 ± 11.55hi	62.96
CS/CEONE	50	50 ± 10bc	25	20 ± 10ab	14.27	70.00 ± 0.0cd	22.22
	100	36.67 ± 5.77cd	45	13.33 ± 5.77abc	42.85	50.00 ± 10.0ef	44.44
	250	30 ± 10de	55	6.67 ± 5.77cd	71.42	36.67 ± 5.77gh	59.26
	500	23.33 ± 5.77e	65	6.67 ± 5.77cd	71.42	30.00 ± 0.0hi	66.67
Flutolanil 25%		20 ± 10e	70	3.33 ± 5.77d	85.71	23.33 ± 5.77i	74.07
Infected control		66.67 ± 5.77a	0	23.33 ± 5.77a	0	90.00a	0
Healthy control		0 ± 0f	100	0 ± 0d	100	0.00	100
LSD		12.19		13.16		12.96	

Note: Values expressed within columns represent the average of three repetitions and means marked with different letters denote significant distinctions (LSD test, $p < 0.05$). Effic. = efficacy. Conc. = concentration.

4 Discussions

The preparation of NEs based on clove oil was achieved in this study through a combination of tween 80, clove oil, and water. Both narrower distribution and decreased size of CS/CEONE can back return to the presence of CS, which is capable of forming a stable charged layer around the oily nanodroplets. Hence, CS acts as a protective layer that prevents the oily nanodroplets from aggregation and enhances the dispersion of nanoparticles within aqueous media, thus maintaining their smaller size [49,50]. A low polydispersity index indicates the uniform size distribution of the developed NE nanodroplets, indicating their stability and

homogeneity [50,51]. Furthermore, the abundance of intense positive charges detected on the surface of the firmulated nanodroplets induces strong repulsive forces that in turn help in the prevention of nanodroplet aggregation and subsequently enhance the overall stability and high dispersibility. These findings agree with those existing in the literature, which stated that the abundance of the substantial amount of surface charges on nanoformulations surfaces contributes to their increased stability [34]. Furthermore, some studies showed that nanoemulsions possessing surface charges over +20 mV or −20 mV are considered highly stable systems owing to the abundance of strong electrostatic repulsion between their oily droplets [52]. The analysis of TEM images revealed that the size measurements obtained were slightly smaller compared to those attained from zeta sizer measurements. This could be attributed to the hydrodynamic effect of abundance of nanoformulations suspended in water compared to the dried samples investigated through TEM analysis [53]. The obtained TEM images reveal great similarity with findings documented in previous literature confirming the successful formation of nanoemulsions with spherical oily nanodroplets [54,55]. CS/CEONE nanodroplets showed a very minute increase in size compared to CEONE. This returns back to the abundance of chitosan with positive charges, forming a shell that prevents the oily nanodroplets aggregation. These findings are conforming with previous literature [22]. It has been reported that keeping the surface charge of nanoformulations exceeding either −20 mV or +20 mV is mandatory to maintain their stability by preventing their aggregation [34,53].

Moreover, both nanoemulsions exhibited an acidic nature, possessing pH values of 5.60 and 5.03, respectively. This finding exhibits great coincidence with previous literature that stated the significance of maintaining the acidic nature of the employed oils in nanoemulsion systems to keep their bioactivity, including antimicrobial features. Moreover, the obtained conductivity measurements for both CEONE and CS/CEONE indicate their thermodynamic stability, confirming their suitability to be stored safely for future applications [56]. According to the UV-Vis spectra results, incorporation of CEO in either CEONE or CS/CEONE systems did not alter the chemical composition of CEO, assuring the convenience of the followed preparation protocol. The results match previous reported studies [57]. The results of CEO release profile demonstrated the sustained and prolonged release from CS/CEONE for up to 4 days. This returns back to the abundance of the swellable chitosan shell surrounding the oily nanodroplets. Our findings are conforming to profiles of previously published chitosan-based nanoformulations [53]. This also matches results obtained for the antifungal activity of CS/CEONE against *R. solani* and *S. rolfsii*, where the antifungal activity was found to extend for a longer time, up to 4 days, compared to the activity of CEONE.

The tested *R. solani* isolates belonging to AG3 exhibited variability in inducing black scurf and stem canker. This variability in virulence can be ascribed to differences in parasitic nature and growth rate [58]. Furthermore, the virulence of *R. solani* isolates in pathogenicity could also be ascribed to the difference between (AGs) [59]. Our results revealed that *R. solani* isolates belonging to AG3 are virulent on potatoes, which is supported by previously reported by Truter et al. [60] who noted that AG3 was more highly virulent than AG4 and AG5. Additionally, Abdel-Sattar et al. [61], found out that AG3 was the dominant and virulent group on potatoes in Egypt. On the other hand, pre-emergence and post-emergence damping-off slightly varied for the five *S. rolfsii* isolates. However, the total pre-emergence and post-emergence damping-off was not significantly varied among the tested isolates. Numerous studies on the pathogenicity of *S. rolfsii* have similarly demonstrated variations in virulence among isolates. For instance, Xie et al. [62] reported variability in virulence among *S. rolfsii* isolates inoculated on tomato and pepper [63] and observed variation in the virulence of 10 *S. rolfsii* isolates on a single tomato variety. Correspondingly, Paparu et al. [5] demonstrated differences in virulence of *S. rolfsii* isolates from the common bean in Uganda.

The *in vitro* and *in vivo* findings confirmed the dose-dependent superiority of CS/CEONE over CEONE and bulk CEO for antifungal effect toward *R. solani* and *S. rolfsii*. In the present study, the maximum

antifungal impact of CS/CEONE over CEONE and bulk CEO was detected at higher concentration of 500 µL/L. This suggests that the encapsulation of CEONE into the chitosan matrix enhanced the inhibitory activity of CEONE. Comparable studies have shown that encasing clove essential oil and *Pepsinum crispum* essential oil into a chitosan nano matrix enhances the antifungal and antioxidant properties [64,65]. Previous studies demonstrated that the nano-encapsulated CEO had a more potent inhibitory effect against *Aspergillus niger*, derived from spoiled pomegranate, in comparison to ChNPs and free oil [66]. Correspondingly, it has been previously reported that *Laurus nobilis* essential oil (LNEO) in chitosan nano matrix exhibited 100% inhibition of *A. flavus* growth at a concentration of 0.4 µL/mL when compared to non-capsulated LENEO, which revealed lower inhibition rate of 70.14% [67]. A more recent study confirmed that the incorporation of *Cymbopogon khasiana* × *Cymbopogon pendulus* EO (CKP-25-EO) into a chitosan nanoemulsion has enhanced its antifungal activity againts *A. humicola*, *A. niger*, *Aspergillus flavus* (AFLHPSc-1), *A. glaucus*, A. luchuensis, *A. spinulosum*, *Penicillium albicans*, and *P. fellutemum* at concentration of 0.08 µL/mL in comparsion with free EO [68]. The previous findings suggest that encapsulating CEONE within a nanostructured system enhanced its antifungal effect [25]. Furthermore, it has been previously proven that chitosan nanoemulsions incorporated with *Eucalyptus citriodora* essential oil had an expressive inhibition rate 73% against *Staphylococcus* aureus [69]. A recently published study indicated that the mixture formula of nanoemulsion of clove oils and black seed significantly suppressed the linear growth of *Alternaria tenuissima*, *Galactomyces candidum* and *Fusarium solani* at 5000 ppm [70]. Moreover, it has been shown that *F. oxysporum* and *R. solani* growth was completely inhibited with clove oil only at the highest concentration of 4% [71]. Likewise, a research study demonstrated that clove oil exhibited a minimum bactericidal concentration (MBC) and MIC of 500 and 400 µL L^{-1}, respectively, against *Pectobacterium carotovorum* subsp. *carotovorum* [72]. Hence, these published findings, along with those reported herein, revealed that essential oils at bulk form poses antifungal activity only when being applied at high concentrations. The treatments of CS/CEONE and CEONE, as well as CEO have significantly decreased the fresh weight of both *R. solani* and *S. rolfsii*, displaying a correlation with the applied dosage. However, this decrease was distinct with the treatment of CS/CEONE especially at high concentrations. Our outcomes concur with those of earlier investigations in which the *Aniba rosaeodora* essential oil encapsulated into chitosan nanoemulsion at concentration 0.6 µL L^{-1} decreased the mycelial fresh weight of *Aspergillus flavus* [73]. It is clear from our results that the inhibitory effect of each CS/CEONE, CEONE, and CEO on the growth of *R. solani* and *S. rolfsii* differed across various fungal genera and species. These results are consistent with prior studies that have reported varying impacts of EOs on different fungi or various isolates of the same species [74,75].

On the other hand, the greenhouse results demonstrated that CS/CEONE and CEONE exhibited an inhibitory activity *vs. R. solani* and *S. rolfsii* over CEO, even at the lowest concentration of 50 µL/L. Our results align with previous research revealed the superiority of nanoemulsions over conventional emulsions. This superiority arises from their increased surface area, reduced size, controlled release of active compounds, and resistance to sedimentation, among other characteristics [76]. Similar to our findings, the utilization of citronella essential oil in nanoemulsion form exhibited notable inhibitory effects at low concentrations against the soil-borne fungi *S. rolfsii* (ED_{50} 14.71 and 20.88 mg L^{-1}) and *R. solani* (ED_{50} 13.67 and 25.64 mg L^{-1}) [77]. Furthermore, an earlier study demonstrated the fungicidal efficacy of eugenol oil nanoemulsion toward *F. oxysporum* f. sp. *vasinfectum*, the pathogen responsible for causing wilt disease in cotton [78]. The very recent study of Attia et al. [79] supported our results of which CEO is very effective in reducing DI of *Rhizoctonia* and *Sclerotium* root rot by 58.33% and 75%, respectively.

In comparison to the untreated control hyphae, the SEM images revealed that the hyphae treated with high concentrations (250 and 500 µL/L) of CS/CEONE and CEONE exhibited distinct alterations in cell

wall structure. Our SEM observations are in accordance with those in the literature, which indicated that the nanoemlusion of *Cleome viscosa* essential oil exhibited also several morphological disruption effects and caused partial cell wall biosynthesis of *Candida albicans* [80]. Furthermore, other studies revealed also that the increased levels of bulck oregano and clove oil caused anomalous cellular structure, including cell membrane rupture and cellular leakage of *Pectobacterium carotovorum* subsp. *carotovorum* [72]. Moreover, a study through SEM micrographs has shown that the nanoemulsion of *Nigella sativa* (black seed) oil provoked morphological changes in the *Penicillium verrucosum* mycelia [81]. Nanoemulsions most likely disrupt protein synthesis and cause membrane instability as their main and secondary antibacterial mechanisms [81]. Nanoemulsions may be absorbed into the cellular DNA binding site, thereby hindering the synthesis of protein and RNA, contributing to their mechanism of action. It was clear from SEM images that the alterations caused by CS/CEONE were superior to CEONE even at low concentrations. These alterations in mycelial morphology could be attributed to the synergistic reaction between CS and CEONE [82]. Our results agree with prior studies indicating that chitosan-loaded nanoemulsions caused atypical conidia formation and the clustering of hyphae in *Colletotrichum gloeosporioides*, which might have contributed to the suppression of enzyme secretion by fungus and ultimately leading to inhibited growth [83].

The crucial role of cellulolytic and pectinolytic enzymes in necrotrophic pathogenesis has been acknowledged, attributing them as significant contributors to infection progression and symptom formation [84]. The effect of CS/CEONE, CEONE and CEO on the production of pectinase and cellulase enzymes of both fungi was evident. In the present study, the most powerful effect was attributed to CS/CEONE, which may be related to the chitosan's antifungal activity. Chitosan possesses the capacity to disrupt the synthesis of toxins specific to the host, as well as organic acids and enzymes responsible for degrading cell walls [85]. The current findings align with previous research demonstrating that the application of chitosan on *A. alternata* resulted in a decrease in the enzymatic activity responsible for cell wall degradation [86]. CEONE and CEO were also effective in inhibiting the effectiveness of pectinase and cellulase enzymes produced by both fungi when compared to control. In a similar study, oregano and clove oils effectively inhibited the excretion of extracellular cell wall degrading enzymes (CWDEs) secreted by *Pectobacterium carotovorum* subsp. *carotovorum*. Remarkably, the activity of pectinase was significantly suppressed (29.82%–100%) [72]. Moreover, it has been proven that the essential oil of *Mentha piperita*, *Bunium persicum* has decreased the effectiveness of cellulase and pectinase produced by *R. solani* and *Macrophomina phaseolina* at low concentrations. So, this suggests that the decreased activity of cellulase and pectinase enzymes in both fungi may contribute to the reduction in their pathogenicity [87].

5 Conclusions

The current study demonstrated that the presence of a chitosan shell encasing the nanodroplets led to a size decrease in their size. Moreover, the existence of a large amount of chitosan resulted in a significant augmentation of the surface charge of the nanodroplets, reaching +25 mV. This confirms chitosan's capacity to enhance the stability of the nanodroplets. This was also evident in the stability studies that demonstrated that CS/CEONE exhibited superior stability regarding size, PDI, surface charge, pH, and conductivity compared to CEONE. The findings demonstrated that the dosage-dependent inhibitory activity of CEONE and CS/CEONE on the mycelial growth of both fungi was seen. In the present work, it was shown that the highest level of antifungal activity was exhibited by CS/CEONE compared to CEONE and bulk CEO at 500 µL/L, indicating that incorporation of CEONE into a chitosan matrix has led to an augmentation of the inhibitory effect of CEONE. The scanning electron microscopy (SEM) photos revealed certain morphological changes, such as crinkling, deformation, and spoiling, in the hyphae of *R. solani* and *S. rolfsii* treated with CEONE and CS/CEONE at concentrations of 500 µL/L. The experimental results clearly demonstrated the influence of CS/CEONE, CEONE, and CEO on the

synthesis of cellulase and pectinase enzymes produced by fungal species. The study concluded that the most significant influence was ascribed to CS/CEONE, potentially associated with the antifungal potential of chitosan. Nanoemulsions originating from essential oil sources are more ecologically sustainable than manufactured fungicides. Nonetheless, their effectiveness and ecological consequences require additional research to optimize dosage, species specificity, ambient conditions, and application methods. Therefore, additional research is necessary to determine whether these nanoemulsions pose health or environmental risks relative to conventional insecticides, as well as to bulk oils, emphasizing their potential toxicity. The validation of the tested nanoemulsions on other plant pathogens and under field conditions could also be investigated in future work.

Acknowledgement: Authors extend their gratitude to the Deanship of Scientific Research, Vice Presidency for Graduate Studies and Scientific Research, King Faisal University, Saudi Arabia, for supporting the current research through grant number KFU241802.

Funding Statement: This research was kindly funded by the Deanship of Scientific Research, Vice Presidency for Graduate Studies and Scientific Research, King Faisal University, Saudi Arabia, grant number (KFU241802).

Author Contributions: Conceptualization, Ahmed Mahmoud Ismail, Eman Said Elshewy and Naglaa Abd Elbaki Sallam Muhanna; methodology, Isra H. Ali, Naglaa Abd Elbaki Sallam Muhanna and Eman Yehia Khafagi; software, Ahmed Mahmoud Ismail and Eman Said Elshewy; validation, Ahmed Mahmoud Ismail and Eman Said Elshewy; formal analysis, Isra H. Ali, Eman Said Elshewy and Naglaa Abd Elbaki Sallam Muhanna; investigation, Eman Yehia Khafag; resources, Isra H. Ali and Naglaa Abd Elbaki Sallam Muhanna; data curation, Eman Said Elshewy; writing—original draft preparation, Isra H. Ali and Ahmed Mahmoud Ismail; writing—review and editing, Ahmed Mahmoud Ismail; visualization, Ahmed Mahmoud Ismail; supervision, Ahmed Mahmoud Ismail; project administration, Ahmed Mahmoud Ismail; funding acquisition, Ahmed Mahmoud Ismail. All authors reviewed the results and approved the final version of the manuscript.

Availability of Data and Materials: The data supporting the findings of this study are available from the corresponding author upon reasonable request.

Ethics Approval: Not applicable.

Conflicts of Interest: The authors declare that they have no conflicts of interest to report regarding the present study.

Supplementary Materials: The supplementary material is available online at https://doi.org/10.32604/phyton.2024.057518.

References

1. Hamza A, Mohamed A, Derbalah A. Unconventional alternatives for control of tomato root rot caused by *Rhizoctonia solani* under greenhouse conditions. J Plant Prot Res. 2016;56(3):298–305. doi:10.1515/jppr-2016-0046.
2. Ismail A. Efficacy of copper oxide and magnesium oxide nanoparticles on controlling black scurf disease on potato. Egypt J Phytopathol. 2021;49(2):116–30. doi:10.21608/ejp.2021.109535.1050.
3. Almaghasla MI, El-Ganainy SM, Ismail AM. Biological activity of four *Trichoderma* species confers protection against *Rhizoctonia solani*, the causal agent of cucumber damping-off and root rot diseases. Sustainability. 2023;15(9):7250. doi:10.3390/su15097250.

4. Carling DE, Kuninaga S, Brainard KA. Hyphal anastomosis reactions, rDNA-internal transcribed spacer sequences, and virulence levels among subsets of *Rhizoctonia solani* anastomosis group-2 (AG-2) and AG-BI. Phytopathology. 2002;92(1):43–50. doi:10.1094/PHYTO.2002.92.1.43.
5. Paparu P, Acur A, Kato F, Acam C, Nakibuule J, Nkuboye A, et al. Morphological and pathogenic characterization of *Sclerotium rolfsii*, the causal agent of southern blight disease on common bean in Uganda. Plant Dis. 2020;104(8):2130–7. doi:10.1094/pdis-10-19-2144-re.
6. Dutta P, Kumari A, Mahanta M, Upamanya GK, Heisnam P, Borua S, et al. Nanotechnological approaches for management of soil-borne plant pathogens. Front Plant Sci. 2023;14:1–15. doi:10.3389/fpls.2023.1136233.
7. Panth M, Hassler SC, Baysal-Gurel F. Methods for management of soilborne diseases in crop production. Agric. 2020;10(1):16. doi:10.3390/agriculture10010016.
8. Allagui MB, Moumni M, Romanazzi G. Antifungal activity of thirty essential oils to control pathogenic fungi of postharvest decay. Antibiotics. 2024;13(1):1–15. doi:10.3390/antibiotics13010028.
9. Tian F, Woo SY, Lee SY, Park SB, Zheng Y, Chun HS. Antifungal activity of essential oil and plant-derived natural compounds against *Aspergillus flavus*. Antibiotics. 2022;11(12):1727. doi:10.3390/antibiotics11121727.
10. Nuñez L, D'Aquino M. Microbicide activity of clove essential oil (*Eugenia caryophyllata*). Brazilian J Microbiol. 2012;43(4):1255–60. doi:10.1590/S1517-83822012000400003.
11. Kumar Pandey V, Shams R, Singh R, Dar AH, Pandiselvam R, Rusu AV, et al. A comprehensive review on clove (*Caryophyllus aromaticus* L.) essential oil and its significance in the formulation of edible coatings for potential food applications. Front Nutr. 2022;9:987674. doi:10.3389/fnut.2022.987674.
12. Naserzadeh Y, Mahmoudi N, Pakina E. Antipathogenic effects of emulsion and nanoemulsion of cinnamon essential oil against *Rhizopus* rot and grey mold on strawberry fruits. Foods Raw Mater. 2019;7(1):210–6.
13. Solans C, Izquierdo P, Nolla J, Azemar N, Garcia-Celma MJ. Nano-emulsions. Curr Opin Colloid Interface Sci. 2005;10(3–4):102–10.
14. McClements DJ. Colloidal basis of emulsion color. Curr Opin Colloid Interface Sci. 2002;7(5–6):451–5.
15. Gulotta A, Saberi AH, Nicoli MC, McClements DJ. Nanoemulsion-based delivery systems for polyunsaturated (ω-3) oils: formation using a spontaneous emulsification method. J Agric Food Chem. 2014;62(7):1720–5. doi:10.1021/jf4054808.
16. Jasrotia P, Nagpal M, Mishra CN, Sharma AK, Kumar S, Kamble U, et al. Nanomaterials for postharvest management of insect pests: current state and future perspectives. Front Nanotechnol. 2022;3:3301. doi:10.3389/fnano.2021.811056.
17. Mustafa IF, Hussein MZ. Synthesis and technology of nanoemulsion-based pesticide formulation. Nanomaterials. 2020;10(8):1608. doi:10.3390/nano10081608.
18. Zhao X, Zhu Y, Zhang C, Lei J, Ma Y, Du F. Positive charge pesticide nanoemulsions prepared by the phase inversion composition method with ionic liquids. RSC Adv. 2017;7(77):48586–96. doi:10.1039/C7RA08653A.
19. McClements DJ, Das AK, Dhar P, Nanda PK, Chatterjee N. Nanoemulsion-based technologies for delivering natural plant-based antimicrobials in foods. Front Sustain Food Syst. 2021;5:1881. doi:10.3389/fsufs.2021.643208.
20. Jesser E, Yeguerman CA, Urrutia RI, Murray AP, Domini C, Werdin-González JO. Development and characterization of nanoemulsions loaded with essential oil and β-cypermethrin and their bioefficacy on insect pest of economic and medical importance. Pest Manag Sci. 2023;79(11):4162–71. doi:10.1002/ps.7613.
21. Pavoni L, Perinelli DR, Bonacucina G, Cespi M, Palmieri GF. An overview of micro- and nanoemulsions as vehicles for essential oils: formulation, preparation and stability. Nanomater. 2020;10(1):135. doi:10.3390/nano10010135.
22. Shetta A, Ali IH, Sharaf NS, Mamdouh W. Review of strategic methods for encapsulating essential oils into chitosan nanosystems and their applications. Int J Biol Macromol. 2024;259:129212. doi:10.1016/j.ijbiomac.2024.129212.
23. Shetta A, Ali IH, Elshishiny F, Mamdouh W. Different approaches for the inclusion of bioactive compounds in packaging systems. In: Jafari SM, Silva AS, editors. Releasing systems in active food packaging: preparation and applications. Cham: Springer International Publishing; 2022. p. 151–85.

24. Beyki M, Zhaveh S, Khalili ST, Rahmani-Cherati T, Abollahi A, Bayat M, et al. Encapsulation of *Mentha piperit*a essential oils in chitosan-cinnamic acid nanogel with enhanced antimicrobial activity against *Aspergillus flavus*. Ind Crops Prod. 2014;54:310–9. doi:10.1016/j.indcrop.2014.01.033.
25. Wang H, Ma Y, Liu L, Liu Y, Niu X. Incorporation of clove essential oil nanoemulsion in chitosan coating to control *Burkholderia gladioli* and improve postharvest quality of fresh *Tremella fuciformis*. LWT. 2022;170: 114059. doi:10.1016/j.lwt.2022.114059.
26. Woranuch S, Yoksan R. Eugenol-loaded chitosan nanoparticles: I. Thermal stability improvement of eugenol through encapsulation. Carbohydr Polym. 2013;96(2):578–85. doi:10.1016/j.carbpol.2012.08.117.
27. Kreutz T, Carneiro SB, Soares KD, Limberger RP, Apel MA, Veiga-Junior VF, et al. *Aniba canelilla* (Kunth) Mez essential oil-loaded nanoemulsion: improved stability of the main constituents and in vitro antichemotactic activity. Ind Crops Prod. 2021;71:113949. doi:10.1016/j.indcrop.2021.113949.
28. Purwanti N, Zehn AS, Pusfitasari ED, Khalid N, Febrianto EY, Mardjan SS, et al. Emulsion stability of clove oil in chitosan and sodium alginate matrix. Int J Food Prop. 2018;21(1):566–81. doi:10.1080/10942912.2018.1454946.
29. Abdel-Naeem HHS, Sallam KI, Malak NML. Improvement of the microbial quality, antioxidant activity, phenolic and flavonoid contents, and shelf life of smoked herring (*Clupea harengus*) during frozen storage by using chitosan edible coating. Food Control. 2021;130:108317. doi:10.1016/j.foodcont.2021.108317.
30. Ale A, Andrade VS, Gutierrez MF, Bacchetta C, Rossi AS, Orihuela PS, et al. Nanotechnology-based pesticides: environmental fate and ecotoxicity. Toxicol Appl Pharmacol. 2023;471:116560. doi:10.1016/j.taap.2023.116560.
31. Heydari M, Amirjani A, Bagheri M, Sharifian I, Sabahi Q. Eco-friendly pesticide based on peppermint oil nanoemulsion: preparation, physicochemical properties, and its aphicidal activity against cotton aphid. Environ Sci Pollut Res. 2020;27(6):6667–79. doi:10.1007/s11356-019-07332-y.
32. Salvia-Trujillo L, Rojas-Graü A, Soliva-Fortuny R, Martín-Belloso O. Physicochemical characterization of lemongrass essential oil-alginate nanoemulsions: effect of ultrasound processing parameters. Food Bioprocess Technol. 2013;6(9):2439–46. doi:10.1007/s11947-012-0881-y.
33. Pramod K, Ilyas UK, Kamal YT, Ahmad S, Ansari SH, Ali J. Development and validation of RP-HPLC-PDA method for the quantification of eugenol in developed nanoemulsion gel and nanoparticles. J Anal Sci Technol. 2013;4(1):1.
34. Ali IH, Khalil IA, El-Sherbiny IM. Single-dose electrospun nanoparticles-in-nanofibers wound dressings with enhanced epithelialization, collagen deposition, and granulation properties. ACS Appl Mater Interfaces. 2016;8(23):14453–69. doi:10.1021/acsami.6b04369.
35. Dellaporta SL, Wood J, Hicks JB. A plant DNA minipreparation: version II. Plant Mol Biol Report. 1983;1(4):19–21. doi:10.1007/BF02712670.
36. White TJ, Bruns TD, Lee SJWTB, Taylor JWL. Amplification and direct sequencing of fungal ribosomal RNA for phylogenetics. In: Innis MA, Gelfand DH, Sninsky JJ, White TJ, editors. PCR protocols: a guide to methods and applications. San Diego, CA: Academic Press; 1990. p. 315–21.
37. Misawa T, Kurose D, Shishido K, Toda T, Kuninaga S. Characterization of a new subgroup of *Rhizoctonia solani* anastomosis group 3 (AG-3 TM) associated with tomato leaf blight. J Gen Plant Pathol. 2020;86(6):457–67. doi:10.1007/s10327-020-00943-1.
38. Tamura K, Stecher G, Kumar S. MEGA11: molecular evolutionary genetics analysis version 11. Mol Biol Evol. 2021;38(7):3022–7. doi:10.1093/molbev/msab120.
39. Abd El-Aziz ARM, Mahmoud MA, AlOthman MR, Abedel-Sattar MA, ElSherif EM, El-Marzouky H. Differential interaction between isolates of *Rhizoctonia solani* AG-3 and potatoes cultivars. Afr J Microbiol Res. 2013;7(12):1045–54.
40. Carling D, Leiner R. Effect of temperature on virulence of *Rhizoctonia solani* and other *Rhizoctonia* on potato. Phytopathology. 1990;80:930–4. doi:10.1094/Phyto-80-930.
41. Hadi MR, Balali G. The effect of salicylic acid on the reduction of *Rizoctonia solani* damage in the tubers of marfona potato cultivar. Am J Agric Environ. 2010;7:492–6.

42. El-Sayed SA, El-Shennawy RZ, Ahmed Mohammed T, Attia AMF. Induction of systemic resistance against damping-off and root-rot of white lupine (*Lupinus albus* L.) using some bioagents, chemical inducers and a mycorrhizal fungus. Casp J Environ Sci. 2022;20(3):571–83.
43. Tatsadjieu NL, Dongmo PMJ, Ngassoum MB, Etoa FX, Mbofung CMF. Investigations on the essential oil of *Lippia rugosa* from Cameroon for its potential use as antifungal agent against *Aspergillus flavus* Link ex. Fries. Food Control. 2009;20(2):161–6. doi:10.1016/j.foodcont.2008.03.008.
44. Montenegro I, Said B, Godoy P, Besoain X, Parra C, Díaz K, et al. Antifungal activity of essential oil and main components from mentha pulegium growing wild on the chilean central coast. Agronomy. 2020;10(2):1–7.
45. Macmillan JD, Vaughn RH. Purification and properties of a polygalacturonic acid-trans-eliminase produced by *Clostridium multifermentans*. Biochemistry. 1964;3(4):564–72. doi:10.1021/bi00892a016.
46. Lorenz MG. Use of dinitrosalicylic acid reagent for determination of reducing sugar. Anal Chem. 1959;31(3):426–8. doi:10.1021/ac60147a030.
47. Snedecor GW, Cochran WG. Statistical methods. 7th ed. Ames, Iowa: Iowa State University Press; 1980.
48. Ellis MB. Illustrated genera of imperfect Fungi. 2nd ed. Minneapolis: Burgess Publishing Company; 1961.
49. Zhao Y, Wang Z, Zhang W, Jiang X. Adsorbed Tween 80 is unique in its ability to improve the stability of gold nanoparticles in solutions of biomolecules. Nanoscale. 2010;2(10):2114–9. doi:10.1039/c0nr00309c.
50. AlMotwaa SM. Coupling Ifosfamide to nanoemulsion-based clove oil enhances its toxicity on malignant breast cancer and cervical cancer cells. Pharmacia. 2021;68(4):779–87. doi:10.3897/pharmacia.68.e68291.
51. Pepper JT, Maheshwari P, Ziemienowicz A, Hazendonk P, Kovalchuk I, Eudes F. Tetrabutylphosphonium bromide reduces size and polydispersity index of Tat_2: siRNA nano-complexes for triticale RNAi. Front Mol Biosci. 2017;4:1–11. doi:10.3389/fmolb.2017.00030.
52. Heurtault B, Saulnier P, Pech B, Proust JE, Benoit JP. Physico-chemical stability of colloidal lipid particles. Biomaterials. 2003;24(23):4283–300. doi:10.1016/S0142-9612(03)00331-4.
53. Ali IH, Elkashlan AM, Hammad MA, Hamdi M. Antimicrobial and anti-SARS-CoV-2 activities of smart daclatasvir-chitosan/gelatin nanoparticles-in-PLLA nanofibrous medical textiles; *in vitro*, and *in vivo* study. Int J Biol Macromol. 2023;253:127350. doi:10.1016/j.ijbiomac.2023.127350.
54. Anjali C, Sharma Y, Mukherjee A, Chandrasekaran N. Neem oil (*Azadirachta indica*) nanoemulsion-a potent larvicidal agent against *Culex quinquefasciatus*. Pest Manag Sci. 2012;68(2):158–63. doi:10.1002/ps.v68.2.
55. Ghosh V, Saranya S, Mukherjee A, Chandrasekaran N. Cinnamon oil nanoemulsion formulation by ultrasonic emulsification: investigation of its bactericidal activity. J Nanosci Nanotechnol. 2013;13(1):114–22. doi:10.1166/jnn.2013.6701.
56. Sh A, AA B, RO M. Nanoemulsion of jojoba oil, preparation, characterization and insecticidal activity against *Sitophilus oryzae* (Coleoptera: curculionidae) on wheat. Int J Agric Innov Res. 2015;4(1):2319–1473.
57. Ayoubi R, Wali S, Singh GB. The UV and FTIR fingerprint of *Ocimum kilimandscharicum* Guerke essential oil: a Eugenol-rich chemo type. Int J Innov Res Sci Stud. 2022;5(1):1–9.
58. Desvani SD, Lestari IB, Wibowo HR, Supyani, Poromarto SH, Hadiwiyono. Morphological characteristics and virulence of *Rhizoctonia solani* isolates collected from some rice production areas in some districts of Central Java. AIP Conf Proc. 2018;2014:020068. doi:10.1063/1.5054472.
59. Yang Y, Zhao C, Guo Z, Wu X. Anastomosis group and pathogenicity of *Rhizoctonia solani* associated with stem canker and black scurf of potato in China. Eur J Plant Pathol. 2015;143(1):99–111. doi:10.1007/s10658-015-0668-x.
60. Truter M, Wehner FC. Anastomosis grouping of *Rhizoctonia solani* associated with black scurf and stem canker of potato in South Africa. Plant Dis. 2004;88(1):83. doi:10.1094/pdis.2004.88.1.83b.
61. Abdel-Sattar M, El-Marzouky H, Ibrahim U. Pathogenicity test and anastomosis group of *Rhizoctonia solani* the causal organism of stem canker and black scurf disease of potato in Egypt. J Appl Plant Prot. 2017;6(1):1–8. doi:10.21608/japp.2017.7494.
62. Xie C, Huang C-H, Vallad GE. Mycelial compatibility and pathogenic diversity among *Sclerotium rolfsii* isolates in the Southern United States. Plant Dis. 2014;98(12):1685–94. doi:10.1094/pdis-08-13-0861-re.

63. Mahato A, Biswas MK. Cultural, morphological and pathogenic variability of different isolates of *Sclerotium rolfsii* obtained from rice-tomato-rice cropping system of undulating red and lateritic zone of West Bengal. Int J Curr Microbiol Appl Sci. 2017;6(3):1843–51. doi:10.20546/ijcmas.2017.603.210.
64. Hadidi M, Pouramin S, Adinepour F, Haghani S, Jafari SM. Chitosan nanoparticles loaded with clove essential oil: characterization, antioxidant and antibacterial activities. Carbohydr Polym. 2020;236:116075. doi:10.1016/j.carbpol.2020.116075.
65. Deepika, Chaudhari AK, Singh A, Das S, Dubey NK. Nanoencapsulated *Petroselinum crispum* essential oil: characterization and practical efficacy against fungal and aflatoxin contamination of stored chia seeds. Food Biosci. 2021;42:101117. doi:10.1016/j.fbio.2021.101117.
66. Hasheminejad N, Khodaiyan F, Safari M. Improving the antifungal activity of clove essential oil encapsulated by chitosan nanoparticles. Food Chem. 2019;275:113–22. doi:10.1016/j.foodchem.2018.09.085.
67. Singh A, Das S, Chaudhari AK, Deepika Soni, Yadav M, Dwivedy A, et al. *Laurus nobilis* essential oil nanoemulsion-infused chitosan: a safe and effective antifungal agent for masticatory preservation. Plant Nano Biol. 2023;5:100043. doi:10.1016/j.plana.2023.100043.
68. Prasad J, Das S, Maurya A, Soni M, Yadav A, Singh B, et al. Encapsulation of *Cymbopogon khasiana* × *Cymbopogon pendulus* essential oil (CKP-25) in chitosan nanoemulsion as a green and novel strategy for mitigation of fungal association and aflatoxin B1 contamination in food system. Foods. 2023;12(4):722. doi:10.3390/foods12040722.
69. Da Silva Abreu FOM, Costa EF, Cardial MRL, André WPP. Polymeric nanoemulsions enriched with *Eucalyptus citriodora* essential oil. Polimeros. 2020;30(2):1–9.
70. Mossa ATH, Mohafrash SMM, Ziedan ESHE, Abdelsalam IS, Sahab AF. Development of eco-friendly nanoemulsions of some natural oils and evaluating of its efficiency against postharvest fruit rot fungi of cucumber. Ind Crops Prod. 2021;159:113049. doi:10.1016/j.indcrop.2020.113049.
71. Thabet M, Khalifa W. Antifungal activities of clove oil against root rot and wilt pathogens of tomato plants. IDOSI Publ. 2018;18(3):105–12.
72. Zhang J, Tian Y, Wang J, Ma J, Liu L, Islam R, et al. Inhibitory effect and possible mechanism of oregano and clove essential oils against *Pectobacterium carotovorum* subsp. *carotovorum* as onion soft rot in storage. Postharvest Biol Technol. 2023;196:112164. doi:10.1016/j.postharvbio.2022.112164.
73. Singh BK, Chaudhari AK, Das S, Tiwari S, Maurya A, Singh VK, et al. Chitosan encompassed *Aniba rosaeodora* essential oil as innovative green candidate for antifungal and antiaflatoxigenic activity in millets with emphasis on cellular and its mode of action. Front Microbiol. 2022;13:1–19.
74. Chang HT, Cheng YH, Wu CL, Chang ST, Chang TT, Su YC. Antifungal activity of essential oil and its constituents from *Calocedrus macrolepis* var. *formosana* florin leaf against plant pathogenic fungi. Bioresour Technol. 2008;99(14):6266–70. doi:10.1016/j.biortech.2007.12.005.
75. Hashem M, Moharam AM, Zaied AA, Saleh FEM. Efficacy of essential oils in the control of cumin root rot disease caused by *Fusarium* spp. Crop Prot. 2010;29(10):1111–7. doi:10.1016/j.cropro.2010.04.020.
76. Mushtaq A, Mohd Wani S, Malik AR, Gull A, Ramniwas S, Ahmad Nayik G, et al. Recent insights into nanoemulsions: their preparation, properties and applications. Food Chem X. 2023;18:100684. doi:10.1016/j.fochx.2023.100684.
77. Osman Mohamed Ali E, Shakil NA, Rana VS, Sarkar DJ, Majumder S, Kaushik P, et al. Antifungal activity of nano emulsions of neem and citronella oils against phytopathogenic fungi, *Rhizoctonia solani* and *Sclerotium rolfsii*. Ind Crops Prod. 2017;108:379–87. doi:10.1016/j.indcrop.2017.06.061.
78. Abd-Elsalam KA, Khokhlov AR. Eugenol oil nanoemulsion: antifungal activity against *Fusarium oxysporum* f. sp. *vasinfectum* and phytotoxicity on cottonseeds. Appl Nanosci. 2015;5(2):255–65. doi:10.1007/s13204-014-0398-y.
79. Attia M, Mohamad A, Baiumy M, Saleh A, Reyad NE-H. Antifungal activity of thyme and clove essential oil nanoemulsions against pothos root rot. Egypt J Agric Sci. 2024;75(2):78–92. doi:10.21608/ejarc.2024.354816.
80. Krishnamoorthy R, Gassem MA, Athinarayanan J, Periyasamy VS, Prasad S, Alshatwi AA. Antifungal activity of nanoemulsion from *Cleome viscosa* essential oil against food-borne pathogenic *Candida albicans*. Saudi J Biol Sci. 2021;28(1):286–93. doi:10.1016/j.sjbs.2020.10.001.

81. Mosa MA, Youssef K, Hamed SF, Hashim AF. Antifungal activity of eco-safe nanoemulsions based on *Nigella sativa* oil against *Penicillium verrucosum* infecting maize seeds: biochemical and physiological traits. Front Microbiol. 2023;13:1–18.
82. Chaudhari AK, Singh VK, Das S, Deepika, Singh BK, Dubey NK. Antimicrobial, aflatoxin B1 inhibitory and lipid oxidation suppressing potential of anethole-based chitosan nanoemulsion as novel preservative for protection of stored maize. Food Bioprocess Technol. 2020;13(8):1462–77. doi:10.1007/s11947-020-02479-w.
83. Zahid N, Ali A, Manickam S, Siddiqui Y, Maqbool M. Potential of chitosan-loaded nanoemulsions to control different *Colletotrichum* spp. and maintain quality of tropical fruits during cold storage. J Appl Microbiol. 2012;113(4):925–39. doi:10.1111/jam.2012.113.issue-4.
84. Prasanth CN, Viswanathan R, Malathi P, Sundar AR. Carbohydrate active enzymes (CAZy) regulate cellulolytic and pectinolytic enzymes in *Colletotrichum falcatum* causing red rot in sugarcane. 3 Biotech. 2022;12(2):1–13.
85. Zahid N, Maqbool M, Ali A, Siddiqui Y, Bhatti QA. Inhibition in production of cellulolytic and pectinolytic enzymes of *Colletotrichum gloeosporioides* isolated from dragon fruit plants in response to submicron chitosan dispersions. Sci Hortic. 2019;243:314–9. doi:10.1016/j.scienta.2018.08.011.
86. Bhaskara Reddy MV, Angers P, Castaigne F, Arul J. Chitosan effects on blackmold rot and pathogenic factors produced by *Alternaria alternata* in postharvest tomatoes. J Am Soc Hortic Sci. 2000;125(6):742–7. doi:10.21273/JASHS.125.6.742.
87. Khaledi N, Taheri P, Tarighi S. Antifungal activity of various essential oils against *Rhizoctonia solani* and *Macrophomina phaseolina* as major bean pathogens. J Appl Microbiol. 2015;118(3):704–17. doi:10.1111/jam.12730.